Viscoelastic properties of demineralized human dentin measured in water with atomic force microscope (AFM)-based indentation

M. Balooch,[1] I-C. Wu-Magidi,[2] A. Balazs,[1] A. S. Lundkvist,[1] S. J. Marshall,[2] G. W. Marshall,[2] W. J. Siekhaus,[1] J. H. Kinney[1]

[1]*Department of Chemistry and Materials Science, Lawrence Livermore National Laboratory, 7000 East Avenue, Livermore, California, 94551*

[2]*Department of Restorative Dentistry, University of California, San Francisco, California 94143*

Abstract: Using an atomic force microscope (AFM) with an attachment specifically designed for indentation, we measured the mechanical properties of demineralized human dentin under three conditions: in water, in air after desiccation, and in water after rehydration. The static elastic modulus (E^h_r = 134 kPa) and viscoelastic responses (τ_ε = 5.1 s and τ_σ = 6.6 s) of the hydrated, demineralized collagen scaffolding were determined from the standard linear solid model of viscoelasticity. No significant variation of these properties was observed with location. On desiccation, the samples showed considerably larger elastic moduli (2 GPa), and a hardness value of 0.2 GPa was measured. Upon rehydration the elastic modulus decreased but did not fully recover to the value prior to dehydration (381 kPa). © 1998 John Wiley & Sons, Inc. *J Biomed Mater Res*, **40**, 539–544, 1998.

Key words: atomic force microscope (AFM); dentin; collagen; viscoelasticity; mechanical properties; elastic modulus

INTRODUCTION

The hardness and elastic modulus of fully mineralized dentin have been reported in many studies. An accepted range in hardness is from 0.2–0.8 GPa.[1–3] The elastic modulus is reported to range between 10–20 GPa.[4–6] Most of the variation in hardness is caused by naturally occurring site-to-site differences in dentin properties.[7,8] The wide variation in the modulus is most likely a combination of these naturally occurring positional variations as well as the difficulty of measuring tissue modulus on small specimens. The range in the reported modulus of dentin is not too dissimilar from that found for cortical bone, which has a similar mineral density.[9]

The elastic modulus of demineralized dentin is of interest because the demineralized collagen network forms the bonding interface in restorative dental procedures that require acid etching.[10,11] However, few studies report a value for the elastic modulus of demineralized dentin. Currey[12] estimated a Young's modulus of bone collagen of 0.12 GPa, an estimate apparently determined from bundled collagen fibrils after preconditioning in tension. Sano, et al.,[3] measured 0.25 GPa on demineralized tensile bar specimens of dentin, but the difficulty of recording small loads required that the modulus be determined at large strain values (10–20% strain) that are not encountered physically. At large strain values, the measurements may be more representative of the compliance of aligned collagen fibrils than they are of the collapsed collagen network that forms the dentin matrix.

In this study, we measured the elastic modulus of fully hydrated demineralized dentin using a modified AFM-based indentation method and small displacements that we believe may better reflect the true compliance of the collagen matrix. The AFM (Nanoscope III, Digital Instruments, Inc., Santa Barbara, CA) was

modified by replacing the conventional head assembly with a transducer-indenter assembly called a Triboscope (Hysitron Inc., Minneapolis, MN). Like its conventional counterpart, the instrument can provide topography mapping of specimens by tracing the superficial contours of the sample with nano-Newton loads. However, unlike the conventional AFM, the device also can be a force-generating and depth-sensing instrument capable of providing load-displacement curves at user-specified locations in ambient and liquid environments. The minimum applied load is less than 1 μN and the maximum displacement that can be measured is 35 μm. Though this is significantly greater than the 1–10 nN loads of the conventional AFM assemblies, the lateral resolution is still the same and is determined by the tip radius. Indenters can be made from a variety of materials (e.g., diamond, tungsten carbide, stainless steel) and can have many shapes (e.g., Berkovich, spherical, flat cylindrical punch) with a range of diameters. The main drawback with the Triboscope is that the large loads can put a signature on soft materials.

MATERIALS AND METHODS

AFM indentation

The Triboscope generates an electrostatic potential between a center pickup electrode and a lower stationary drive plate. This potential generates an attraction force that drives the center pickup electrode toward the drive plate. An indenter rigidly attached to the center pickup electrode transfers this force to a sample mounted on the Piezo tube scanner of the AFM (Fig. 1). From the known plate separation, the force can be calculated from the potential that is applied between the plates. At the same time, the electrode (tip) displacement can be measured from a DC voltage that is
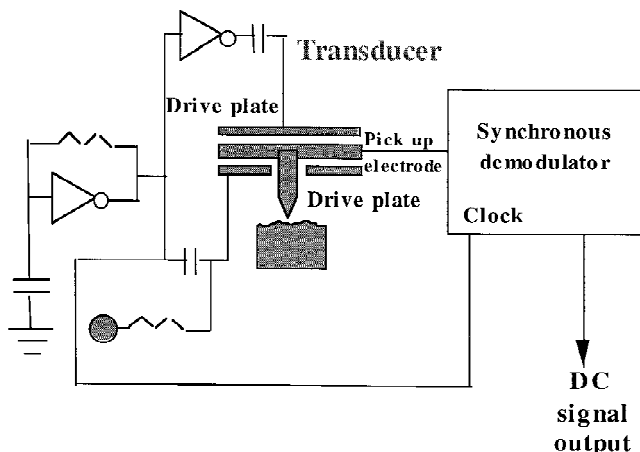
Figure 1. Schematic diagram of transducer and circuit drive.

proportional to the pickup electrode displacement. In the conventional AFM mode, this DC voltage is used as the feedback for constant force mode imaging. In the indenter mode, this DC voltage is used to measure the tip displacement.

The detailed components of the instrument are shown in Figure 1. In the instrument, as provided by the company, the force that is recorded and displayed is calculated by:

$$F_{display} = \frac{A}{2} \varepsilon_0 \frac{v^2}{d_0^2} \qquad (1)$$

where A is the plate area, v is the applied voltage between the drive plate and pickup electrode, ε_0 is the dielectric constant of air, and d_0 is the spacing between the pickup electrode and the drive plate when no weight (such as the indenter) is attached and no voltage is applied. For most applications, Equation (1) adequately calculates the force applied to the material. For soft materials, however, the displacements can be large even for small applied voltages. In these cases, the force that is displayed by the instrument does not equal the force actually applied to the sample because for large displacements the stiffness of the membrane, which is necessary for providing a restoring force to the tip assembly, needs to be considered. Also, for applications in liquid, the weight of the indenter and the force exerted on the indenter's shaft as a result of surface tension must be included.

The actual force applied to the sample (ignoring possible nonlinearity in the spring constant of the membrane) is

$$F_a = F_{display} \left[\frac{d_0}{d^{in} - x} \right]^2 - K_s(x + d_0 - d_{in}) + F_{s.t.} + mg \qquad (2)$$

where x is the displacement of the pickup electrode from its initial position d^{in}, K_s is the spring constant of the membrane, mg is the weight of the indenter, and $F_{s.t.}$ is the force due to surface tension between the indenter and the liquid (see Fig. 2). In the absence of initial loading, the initial spacing, d^{in}, is

$$d^{in} = d_1^{air} - \frac{F_{s.t.}}{K_s} \qquad (3)$$

where d_1^{air} is the spacing between the pickup electrode and the drive plate in air, which is different from d_0 due to the weight of the attached indenter. In these equations, d_0 is specified by the vender (120 μm), and d_1^{air}, $F_{s.t.}$, and K_s are determined by making a best fit to the displayed force versus distance curves of several calibration runs done in air and liquid without a sample. The results are shown in Figure 3(a) along with an expanded scale showing the deviation of experimental points from the optimum fit. The experiments were repeated in liquid with no load to obtain $F_{s.t.}$. The result of the curve fit and its deviation from data points in water are shown in Figure 3(b).

The "sine wave" appearance of the deviation of experimental results from the optimum fit to curves of force versus displacement, evident in both air and liquid calibration runs, can be eliminated when a nonlinear third-power term, as suggested by Timoshenko and Goodier,[13] is added to describe the force versus displacement of the membrane. The load accuracy of the measurements without this correction,
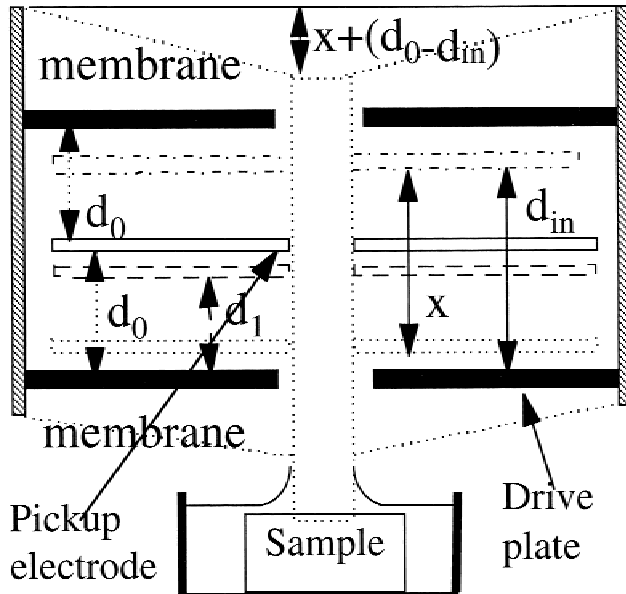
Figure 2. Detailed operation of transducer components with parameters needed to determine the actual force applied to a soft material in water.

however, is better than ± 10 μN in air and ± 20 μN in water. Therefore, in this study the nonlinear spring correction was not used.

Specimen preparation

Saggital sections with a buccolingual orientation were prepared from the coronal dentin of three freshly extracted third molars. The teeth were sterilized with gamma irradiation.[14] The 1-mm thick dentin sections were polished, to remove the smear layer, and demineralized in 0.5M EDTA at pH 7.4 for 3 days. After demineralization, the samples were stored in deionized water at 4°C until studied with the AFM. After making the initial indentation measurements on the hydrated dentin specimens, the samples were desiccated in a vacuum of 10^{-3} Torr pressure for 30 min with a mechanical pump. The desiccated specimens were studied in air with the AFM and then stored dry for 7 days prior to rehydration. The specimens were rehydrated in deionized water for 24 h and then reanalyzed with the AFM.

Experimental procedure

The specimens were indented at three locations: near the dentinoenamel junction, in the midcoronal dentin, and near the pulp. Because demineralized dentin preserved in liquid was suspected to have low elastic modulus, a flat circular punch rod 170 μm in diameter was used. The instrument was programmed to generate a trapezoidal force versus time profile. The data were analyzed using a standard linear solid model:[15] a spring (μ_0) placed in parallel with a Maxwell spring (μ_1)-damper (η_1) couple. A second order polynomial
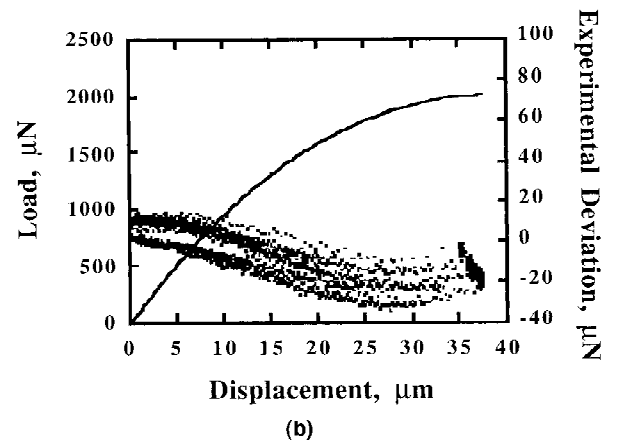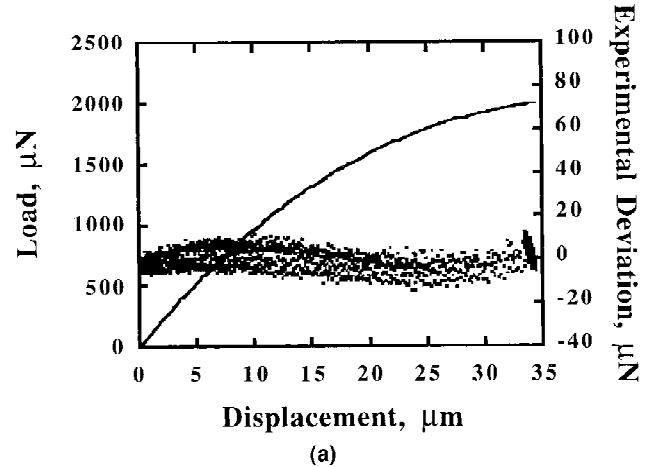
Figure 3. Force versus displacement with no load, and deviation of experimental results from the optimum fit to force versus displacement: (a) air; (b) water.

was fit to the *loading portion* of the applied force versus time curve, and this fitted analytic function then was integrated using the Boltzmann superposition principle for creep response given an arbitrary load profile. This resulted in an analytic function, X(t), containing the undetermined standard linear model parameters E_r (relaxed elastic modulus), τ_ε (relaxation time constant for constant strain), and τ_σ (the relaxation time constant for constant stress). These parameters then were determined from a best fit of X ($t,E_r,\tau_\varepsilon,\tau_\sigma$) with the measured displacement during the loading portion of the displacement versus time data.[16]

Because the desiccated specimens were much stiffer, a pyramidal diamond tip with a 50 nm radius of curvature replaced the circular punch for those measurements. Also, because desiccated dentin was no longer viscoelastic, the elastic modulus was calculated from the contact stiffness defined as the slope of the force/displacement curve during unloading:[17]

$$E = \frac{\sqrt{\pi}}{2\sqrt{a}} S \qquad (5)$$

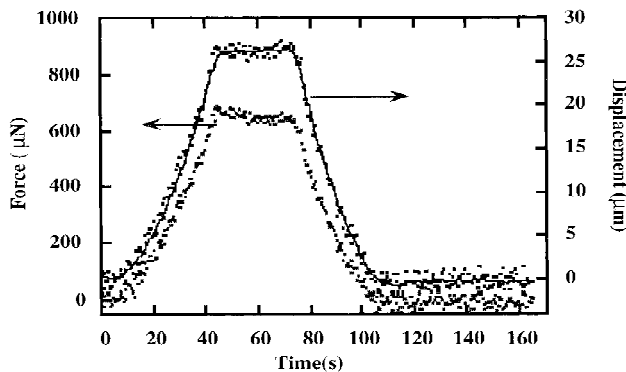and hardness was determined as:

$$H = \frac{F_{max}}{a} \qquad (6)$$

where S was the contact stiffness, F_{max} was the maximum load, and a was the projected contact area while the load was applied. Hardness could not be measured in the fully hydrated dentin specimens because no permanent deformation could be detected.

A major source of error in measurements of this kind is tip area uncertainty. The circular punch was chosen because the contact area was independent of displacement, thereby providing a constant circumference to eliminate depth-dependent variations in the surface tension between the liquid and punch. The area of the pyramidal punch was calibrated by indenting fused silica of known hardness and modulus to similar depths used in this study.

RESULTS

The nearly trapezoidal force and resulting displacement behavior are shown as a function of time in Figure 4 for a typical demineralized specimen. The viscoelastic constants defined by the standard linear model are provided in Table I for the demineralized specimens. To check the validity of these parameters, the displacement behavior due to a nearly square force was studied on one of the samples [Fig. 5(a)]. A sum of exponentials approximated a force function expressing the best fit to the force versus time data. The results near maximum force and predicted displacement are given in Figure 5(b), suggesting a good agreement between the data and the standard linear model. It is worth emphasizing that the behavior of the demineralized material is nearly elastic, as can be seen from both Figures 4 and 5.

A typical force displacement curve for desiccated specimens is shown in Figure 6. The hardness and

TABLE I
Original Demineralized Dentin Mechanical Properties

Sample #	517	670	671
E_r (KPa)	132.7	151.0	162.3
τ_ε (s)	4.77	5.23	5.20
τ_σ (s)	6.06	6.63	7.10

elastic modulus did not change appreciably with different maximum loads. The average values of E and H for the three desiccated specimens are shown in Table II.

The standard linear model parameters for the rehydrated specimens are provided in Table III. The elastic moduli reduced drastically from the desiccated state; however, they did not recover to their original values. The characteristic times, τ_ε and τ_σ, were reduced by about a factor of two in the rehydrating process. Dis-

(a)
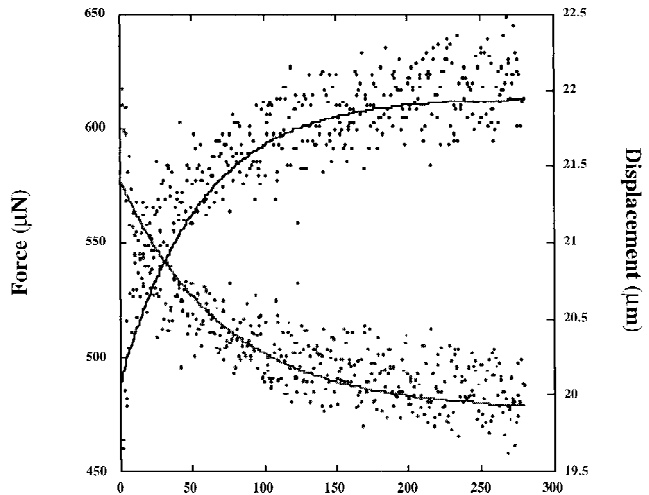
(b)

Figure 5. The nearly square force and resulting displacement behavior as a function of time. The lines are predictions of the standard linear model with the same parameters used for the trapezoidal force.
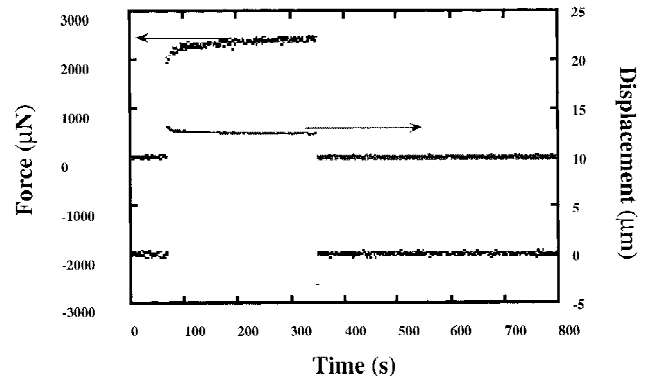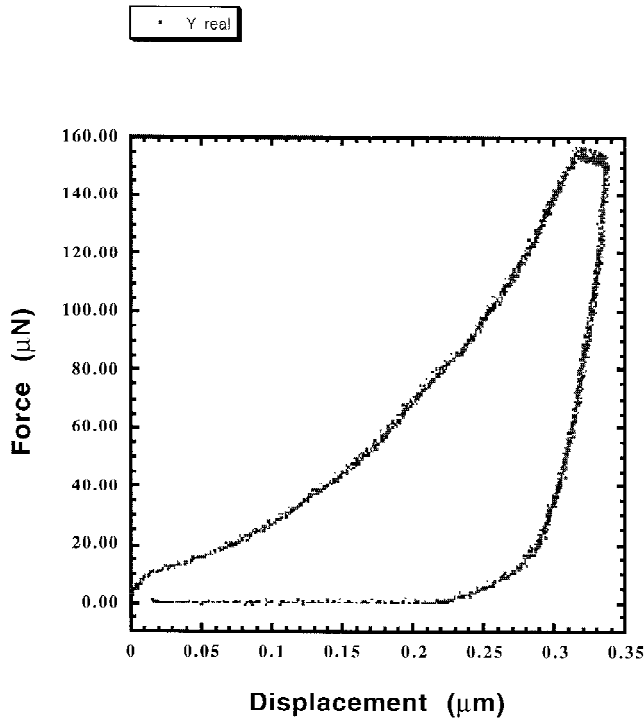

Figure 4. The nearly trapezoid force and resulting displacement behavior as a function of time. The line fit to the displacement data represents the prediction of the standard linear model with parameters reported in Table I.

Figure 6. Force-displacement curve of dehydrated specimen #671.

coloration of the dentin (it became a tan color) was noted after storage in air for several days.

A two-way ANOVA with Tukey's multiple comparison test showed there to be no significant difference with intratooth position ($p < .05$) for either modulus or time constants. All treatment groups (hydrated, desiccated, rehydrated) had significantly different moduli.

DISCUSSION

The results of our study confirm that collagen contributes virtually nothing to dentin modulus although it is a significant contributor to dentin strength and toughness.[3] Furthermore, within experimental error, there was no detectable difference in modulus between the collagen near the dentinoenamel junction and collagen near the pulp. This means that observed differences in hardness and modulus with intratooth position in fully mineralized dentin must be due to

TABLE II
Elastic Modulus and Hardness of Dehydrated Samples

Sample #	517	670	671
E (GPa)	2.3	1.9	2.1
H (GPa)	0.22	0.18	0.20

TABLE III
Viscoelastic Properties of Rehydrated Demineralized Dentin

Sample #	517	670	671
E_r (KPa)	387.3	366.8	390.0
τ_ε (s)	2.57	2.83	3.28
τ_σ (s)	2.90	3.39	3.35

differences in mineral concentration and not to altered collagen properties.

Many bonding procedures in restorative dentistry rely on acid etching and drying of the exposed collagen surface.[10] Therefore, the recovery of the elastic modulus after dehydration is of importance in adhesion and bonding to the etched dentin surface. After several days in air storage, the demineralized dentin specimens began to discolor. We believe that this discoloration indicated that some amount of oxidation-induced cross linking of the collagen had occurred. We hypothesize that oxidation-induced cross linking and possible chain entanglement during drying were responsible for the lack of full recovery on rehydration. The rehydrated specimens had more than two times the modulus in all cases, but this still was insignificant with respect to the modulus of fully mineralized dentin.

Our results indicate that fully demineralized dentin behaves viscoelastically: no plastic deformation was detectable after the loads were removed. The modulus values obtained in our study were more than 1000 times smaller than reported previously (0.25 GPa). Previous measurements, however, were made in tension at large strains. Because dentin collagen looks like a woven mat, tensile forces will unkink the fibers gradually over time, changing the structure to a more highly aligned configuration. We therefore would not expect to see a modulus that is independent of strain, as was pointed out over three decades ago by Currey.[12] In addition, we might expect to see longer relaxation times at high tensile loads; indeed, stress relaxation times of greater than a thousand seconds have been reported for demineralized bone specimens in tension.[18]

In summary, the standard linear solid model predicted the viscoelastic response of demineralized dentin in the small strain limit. With desiccation, the demineralized dentin no longer was viscoelastic and had a modulus value that was over four orders of magnitude greater than that of hydrated demineralized dentin. The modulus did not fully recover upon rehydration, most likely because of the residual effects of oxidation-induced crosslinking and chain entanglement of the collagen during drying.

References

1. T. Fusayama and T. Maeda, ''Effect of pulpectomy on dentin hardness,'' *J. Dent. Res.,* **48**, 452–460 (1969).

2. D. Pashley, A. Okabe, and P. Parham, ''The relationship between dentin microhardness and tubule density,'' *Endo. Dent. Traumatol.,* **1**, 176–179 (1985).

3. H. Sano, B. Ciucchi, W. G. Matthews, and D. H. Pashley, ''Tensile properties of mineralized and demineralized human and bovine dentin,'' *J. Dent. Res.,* **73**, 1205–1211 (1994).

4. R. L. Bowen and M. M. Rodriguez, ''Tensile and modulus of elasticity of tooth structure and several restorative materials,'' *J. Am. Dent. Assoc.,* **64**, 378–387 (1962).

5. R. G. Craig and F. A. Peyton, ''Elastic and mechanical properties of human dentin,'' *J. Dent. Res.,* **37**, 710–718 (1958).

6. M. L. Lehmann, ''Tensile strength of human dentin,'' *J. Dent. Res.,* **46**, 197–201 (1967).

7. J. H. Kinney, M. Balooch, S. J. Marshall, G. W. Marshall, and T. P. Weihs, ''Hardness and Young's modulus of human peritubular and intertubular dentine,'' *Arch. Oral Biol.,* **41**, 9–13 (1996a).

8. J. H. Kinney, M. Balooch, S. J. Marshall, G. W. Marshall, and T. P. Weihs, ''Atomic force microscope measurements of the hardness and elasticity of peritubular and intertubular human dentin,'' *J. Biomech. Eng.,* **188**, 133–135 (1996b).

9. T. M. Keaveny and W. C. Hayes, ''A 20-year perspective on the mechanical properties of trabecular bone,'' *J. Biomech. Eng.,* **115**, 534–542 (1993).

10. N. Nakabayashi, K. Kojima, and E. Masuhara, ''The promotion of adhesion by the infiltration of monomers into tooth substrates,'' *J. Biomed. Mater. Res.,* **16**, 265–273 (1982).

11. B. van Meerbeek, G. Willems, J. P. Celis, J. R. Roos, M. Braem, P. Lambrechts, and G. Vanherle, ''Assessment by nanoindentation of the hardness and elasticity of the resin dentin bonding area,'' *J. Dent. Res.,* **72**, 1434–1442 (1993).

12. J. D. Currey, ''Three analogies to explain to explain the mechanical properties of bone,'' *Biorheol.,* **2**, 1–10 (1964).

13. S. P. Timoshenko and J. N. Goodier, *Theory of Elasticity,* 3rd ed., McGraw–Hill, Inc., New York, 1970.

14. J. M. White, H. E. Goodis, S. J. Marshall, and G. W. Marshall, ''Sterilization of teeth by gamma radiation,'' *J. Dent. Res.,* **73**, 1560–1567 (1994).

15. Y. C. Fung, *Biomechanics,* 2nd ed., Springer–Verlag, New York, 1993, pp. 41–46.

16. A. Lundkvist, E. Lilleodden, W. J. Siekhaus, J. H. Kinney, L. Pruitt, and M. Balooch, ''Viscoelastic properties of healthy human artery measured in saline solution by AFM-based indentation technique,'' in *Conference Proceedings of the Materials Research Society: Thin Films—Stress and Mechanical Properties,* VL, **436**, 353–358 (1996).

17. M. F. Doerner and W. D. Nix, ''A method for interpreting the data from depth-sensing indentation measurements,'' *J. Mater. Res.,* **1**, 601–609 (1986).

18. N. Sasaki, Y. Nakayama, M. Yoshikawa, and E. Atsushi, ''Stress relaxation function of bone and bone collagen,'' *J. Biomech.,* **26**, 1369–1376 (1993).